

Published in final edited form as:

Chem Commun (Camb). 2011 August 14; 47(30): 8620–8622. doi:10.1039/c1cc12981c.

Multivalent Glyconanoparticles with Enhanced Affinity to the Anti-Viral Lectin Cyanovirin-N

Xin Wang^{a,†}, Elena Matej^{b,†}, Lingquan Deng^{c,†}, Olof Ramström^c, Angela M. Gronenborn^b, and Mingdi Yan^a

Olof Ramström: ramstrom@kth.se; Angela M. Gronenborn: amg100@pitt.edu; Mingdi Yan: yanm@pdx.edu

^aDepartment of Chemistry, Portland State University, P.O. Box 751, Portland, Oregon, 97207-0751 USA. Fax: 01 5037259525; Tel: 01 5037255756

^bDepartment of Structural Biology, University of Pittsburgh Medical School, Pittsburgh, PA 15260. USA. Tel: 01 4126489959

^cDepartment of Chemistry, KTH - Royal Institute of Technology, Teknikringen 30, S-10044 Stockholm, Sweden. Fax: 46 87912333; Tel: 46 87906915

Abstract

Low-mannose (LM) structures were coupled to gold nanoparticles (Au NPs) to amplify the affinity of LMs with Cyanovirin-N (CV-N) lectins and to study the structures of CV-N variants CVN^{Q50C} and CVN^{MutDB}.

Lectins, carbohydrate-binding proteins, play critical roles in a plethora of biological processes.¹ An in-depth understanding of carbohydrate-lectin interactions is not only fundamentally important for elucidating their biological functions, but also of outstanding practical value in the design and development of therapeutics and diagnostic tools. CV-N is an 11 kDa cyanobacterial lectin that exhibits inhibitory activity against a number of viruses, including HIV, at concentrations as low as nanomolar. Its anti-HIV activity is mediated by binding to the high-mannose (HM) structures on the envelope glycoprotein gp120.²⁻⁶ Previous studies established that the binding epitope(s) on *N*-linked high oligomannosides for CV-N comprised -D-Man_p-(1 → 2)- -D-Man_p moieties on the glycan's D1 and D3 arms.⁷⁻¹⁰

Multivalency, resulting in cooperative interactions of multiple ligands with multiple receptors, is a general phenomenon that occurs in many biological processes involving molecular recognition. Multivalent interactions are often significantly stronger than the corresponding monovalent interactions, and, as such, the design and creation of multivalent reagents is an important strategy for generating diagnostic and therapeutic tools.¹¹ In glycobiology, these kinds of approaches are especially relevant given the commonly observed weak affinities between glycans and lectins.^{12, 13} On the other hand, high glycan structures exhibit drastically enhanced apparent affinities, compared to the monovalent ligands. However, the synthesis of high glycans is tremendously demanding, involving multiple protection/deprotection steps and complex stereochemistry control. As such, their

© The Royal Society of Chemistry [2011]

Correspondence to: Olof Ramström, ramstrom@kth.se; Angela M. Gronenborn, amg100@pitt.edu; Mingdi Yan, yanm@pdx.edu.

[†]These authors contributed equally to this work.

[†]Electronic Supplementary Information (ESI) available: Experimental details, nanoparticle characterization, ITC results. See DOI: 10.1039/b000000x/

availability is limited. An alternative approach for creating multivalency is to use a scaffold, such as polymers, lipids or nanomaterials, on which multiple copies of a ligand can be presented, thereby generating a multivalent ligand.¹⁴⁻¹⁷ For example, Melander and coworkers prepared small molecule-coated AuNPs as effective inhibitors for HIV fusion,¹⁸ and Gervay-Hague's group reported that galactosyl- and glucosyl-functionalized AuNPs exhibited 300 times better binding to gp120.¹⁹ In previous studies from our group, we showed that carbohydrate ligands conjugated to AuNPs exhibited affinities up to five orders of magnitude higher than those of the corresponding monomeric ligands with lectins.²⁰

Here, we conjugated two low-mannoses, Man2 and Man3, to the AuNP scaffold, and investigated the binding affinity of the resulting GNPs with CV-N lectins (Fig. 1). In order to derive quantitative numbers for the affinity enhancement caused by AuNPs, we developed a fluorescence competition assay and determined the apparent dissociation constant of GNP binding to CV-N (K_D). The results from this assay were compared with the K_D values of monomeric glycan binding to CV-N using isothermal titration calorimetry (ITC).

GNP-M2 and **GNP-M3** were prepared following a previously established procedure,²¹ outlined in Fig. 1. Uniform, ~22 nm AuNPs were synthesized by the Turkevich method²² and were subsequently functionalized with PFPA-disulfide (Fig. 1). Man2 and Man3 were then conjugated to the PFPA-functionalized AuNPs using a photocoupling method²¹ (see details in ESI†) by way of a CH insertion reaction of the photogenerated perfluorophenyl nitrene.^{23, 24} The ligand density was determined using a colorimetric approach with anthrone/sulfuric acid. Values of $1,516 \pm 232$ Man2 and $1,037 \pm 148$ Man3 were obtained for **GNP-M2** and **GNP-M3**, respectively.

Binding affinities of **GNP-M3** to CV-N was evaluated using two CV-N variants: CVN^{MutDB} and CVN^{Q50C}. CVN^{Q50C} is essentially a wild-type variant, comprising two separate glycan binding sites one on Domain A and one on Domain B.^{8, 10} Domain A exhibits a slight preference for the Man3 units and domain B for the Man2 units.^{10, 25} The Cys substitution at position 50 was introduced to allow for specific fluorescence labeling of CV-N without interfering with glycan binding. In the CVN^{MutDB} variant on the other hand, the glycan binding site on domain B is completely eliminated, while the site on domain A still can bind glycan ligands. Since this variant no longer can cross-link glycans on gp120, it has lost its anti-HIV activity.²⁶ Therefore, in interactions with GNPs, we would expect that CVN^{Q50C} can act as a crosslinker and form a complex with **GNP-M3**, while no such crosslinking should be possible between **GNP-M3** and CVN^{MutDB}. Indeed, **GNP-M3** treatment with CVN^{Q50C} caused a red shift from 529 nm to 542 nm in the surface plasmon resonance (SPR) band of AuNPs (Fig. 2a), indicative of particle size growth.²⁷ Such an increase in particle size was further confirmed by TEM which revealed the presence of clusters of aggregated particles (Fig. 2c). When **GNP-M3** was treated with CVN^{MutDB}, however, no SPR shift was observed (Fig. 2b). TEM images were devoid of aggregates and only isolated single particles were observed in this case (Fig. 2c). Dynamic light scattering (DLS) measurements of CV-N treated **GNP-M3** particles yielded average particle sizes of 25.9 ± 3.5 nm and 38.3 ± 4.6 nm for CVN^{MutDB} and CVN^{Q50C}, respectively (Fig. 2S, ESI†). These results are all consistent with our previous structural studies on CVN^{MutDB} that revealed a single glycan binding site.²⁶

The binding affinities of the GNPs to the CV-N variants were evaluated using a recently developed fluorescence-based competition assay.²⁰ In the experiment, free ligand competitor (Man2 for **GNP-M2**, Man3 for **GNP-M3**) together with varying concentrations of **GNP-M2** or **GNP-M3** was incubated at a fixed concentration of Cy5-CVN^{Q50C}, specifically Cy5-labeled CVN^{Q50C} (Fig. 3a, see ESI† for experimental details). The solution was centrifuged to remove all GNPs and the fluorescence intensity of the supernatant was

measured. The difference in fluorescence intensity of Cy5-CVN^{Q50C} before and after incubation with GNPs corresponds to the amount of the bound CVN^{Q50C}. Concentration response curves for **GNP-M2** or **GNP-M3** permit the determination of IC₅₀ values (Fig. 3c).

In order to extract the binding constants of GNPs with CVN^{Q50C}, it is necessary to know the K_d values of the monomeric ligands, Man2 and Man3, with CVN^{Q50C} (Fig. 3b). These values were determined by ITC and the dissociation constants, K_{d1} (glycan-binding site on Domain A) and K_{d2} (glycan-binding site on Domain B), were calculated based on a two-site binding model (see ESI† for details). Values for K_{d1} and K_{d2} of 700 μM and 64 μM for Man2, and 3.4 μM and 43 μM for Man3, respectively, were calculated (Table 1). These values agree well with our previous observation that slightly stronger binding of Man2 to the site on Domain B than to that on Domain A occurs, while the opposite is true for Man3.^{8, 10, 26} These data, together with the IC₅₀ values determined from the data shown in Fig. 3c, were then used to calculate the apparent dissociation constants for the site on Domain B, K_{D1} and K_{D2}, based on a two binding site model (Fig. 3b, see ESI† for details). The data summarized in Table 1 demonstrate that both GNPs, **GNP-M2** and **GNP-M3**, exhibit an affinity enhancement by several orders of magnitude compared to the affinities measured for the isolated, monomeric sugars interacting with CVN^{Q50C}. Taking into account the number of ligands on the particles, i.e. considering the affinity/ligand, an increase up to several hundred times is still present for the AuNP-bound glycan (Table 1). In addition, **GNP-M3** exhibited a higher affinity than **GNP-M2** for both domains. These results correlate well with the general affinity ranking of the free ligands Man2 and Man3, and are consistent with observations in our previous study with a different GNP-lectin system.²⁰ Interestingly, for both **GNP-M2** and **GNP-M3**, the affinity enhancement is more pronounced for the better binding domain. For example, Man2 exhibits a higher affinity for the binding site on Domain B, and with **GNP-M2**, the affinity enhancement factor (EF) is 178 for the Domain B site vs. 8.3 for the Domain A site (Table 1). For **GNP-M3**, on the other hand, the opposite was observed that the EF is higher for the Domain A site (340) than for the Domain B site (3.8).

In conclusion, we have successfully grafted low-mannose ligands onto AuNPs via an efficient photocoupling reaction. The resulting GNPs interacted with the CV-N variants CVN^{MutDB} and CVN^{Q50C} in a manner that is consistent with the expected behavior of one- and two-site binders. Crosslinked complexes and aggregates were observed when **GNP-M3** was treated with the two-site CVN^{Q50C} while only single particles were seen after treatment with the single-site variant CVN^{MutDB}. Furthermore, these GNPs exhibited significantly higher affinity towards the CV-N lectins, compared to the free glycan ligands, demonstrating that AuNPs serve as an efficient multivalent scaffold that significantly enhances the apparent affinity. This affinity enhancement compares well with that of other synthetic multivalent ligands. Therefore, a general strategy can be envisioned which uses simple glycans, rather than large and complex sugars, for grafting onto a multivalent scaffold for affinity amplification. These types of approaches will aid in development of effective new glyconanomaterials for diagnostic and therapeutic applications.

Supplementary Material

Refer to Web version on PubMed Central for supplementary material.

Acknowledgments

This work was supported National Institutes of Health Grants R01GM080295 and 2R15GM066279 (to M.Y.) and R01GM080642 (to A.M.G.). LD thanks the China Scholarship Council for a special scholarship award.

References

1. Lis H, Sharon N. *Chem Rev.* 1998; 98:637–674. [PubMed: 11848911]
2. Bewley CA, Gustafson KR, Boyd MR, Covell DG, Bax A, Clore GM, Gronenborn AM. *Nat Struct Biol.* 1998; 5:571–578. [PubMed: 9665171]
3. Choi, SK. *Synthetic multivalent molecules : concepts and biomedical applications.* John Wiley & Sons, Inc.; Hoboken, New Jersey: 2004. p. 53-63.
4. Liu YA, Carroll JR, Holt LA, McMahon J, Giomarelli B, Ghirlanda G. *Biopolymers.* 2009; 92:194–200. [PubMed: 19235857]
5. O'Keefe BR, Shenoy SR, Xie D, Zhang WT, Muschik JM, Currens MJ, Chaiken I, Boyd MR. *Mol Pharmacol.* 2000; 58:982–992. [PubMed: 11040045]
6. Shenoy SR, O'Keefe BR, Bolmstedt AJ, Cartner LK, Boyd MR. *J Pharmacol Exp Ther.* 2001; 297:704–710. [PubMed: 11303061]
7. Barrientos LG, Gronenborn AM. *Mini-Rev Med Chem.* 2005; 5:21–31. [PubMed: 15638789]
8. Bewley CA, Otero-Quintero S. *J Am Chem Soc.* 2001; 123:3892–3902. [PubMed: 11457139]
9. Bolmstedt AJ, O'Keefe BR, Shenoy SR, McMahon JB, Boyd MR. *Mol Pharmacol.* 2001; 59:949–954. [PubMed: 11306674]
10. Shenoy SR, Barrientos LG, Ratner DM, O'Keefe BR, Seeberger PH, Gronenborn AM, Boyd MR. *Chem Biol.* 2002; 9:1109–1118. [PubMed: 12401495]
11. Mammen M, Choi SK, Whitesides GM. *Angew Chem Int Ed.* 1998; 37:2754–2794.
12. Dam TK, Brewer CF. *Glycobiology.* 2010; 20:270–279. [PubMed: 19939826]
13. Lee YC, Lee RT. *Acc Chem Res.* 1995; 28:321–327.
14. Jayaraman N. *Chem Soc Rev.* 2009; 38:3463–3483. [PubMed: 20449063]
15. Lim Y, Lee M. *Org Biomol Chem.* 2007; 5:401–405. [PubMed: 17252119]
16. Shenhar R, Rotello VM. *Acc Chem Res.* 2003; 36:549–561. [PubMed: 12859216]
17. Wang X, Ramström O, Yan M. *Adv Mater.* 2010; 22:1946–1953. [PubMed: 20301131]
18. Bowman MC, Ballard TE, Ackerson CJ, Feldheim DL, Margolis DM, Melander C. *J Am Chem Soc.* 2008; 130:6896–6897. [PubMed: 18473457]
19. Nolting B, Yu JJ, Liu GY, Cho SJ, Kauzlarich S, Gervay-Hague J. *Langmuir.* 2003; 19:6465–6473.
20. Wang X, Ramström O, Yan M. *Anal Chem.* 2010; 82:9082–9089.
21. Wang X, Ramström O, Yan M. *J Mater Chem.* 2009; 19:8944–8949. [PubMed: 20856694]
22. Turkevich J, Stevenson PC, Hollier J. *Discuss Faraday Soc.* 1951; 11:55–75.
23. Liu LH, Yan M. *Acc Chem Res.* 2010; 43:1434–1443. [PubMed: 20690606]
24. Wang X, Liu LH, Ramström O, Yan MD. *Exp Biol Med.* 2009; 234:1128–1139.
25. Bewley CA, Kiyonaka S, Hamachi I. *J Mol Biol.* 2002; 322:881–889. [PubMed: 12270721]
26. Matei E, Furey W, Gronenborn AM. *Structure.* 2008; 16:1183–1194. [PubMed: 18682220]
27. Daniel MC, Astruc D. *Chem Rev.* 2003; 104:293–346. [PubMed: 14719978]

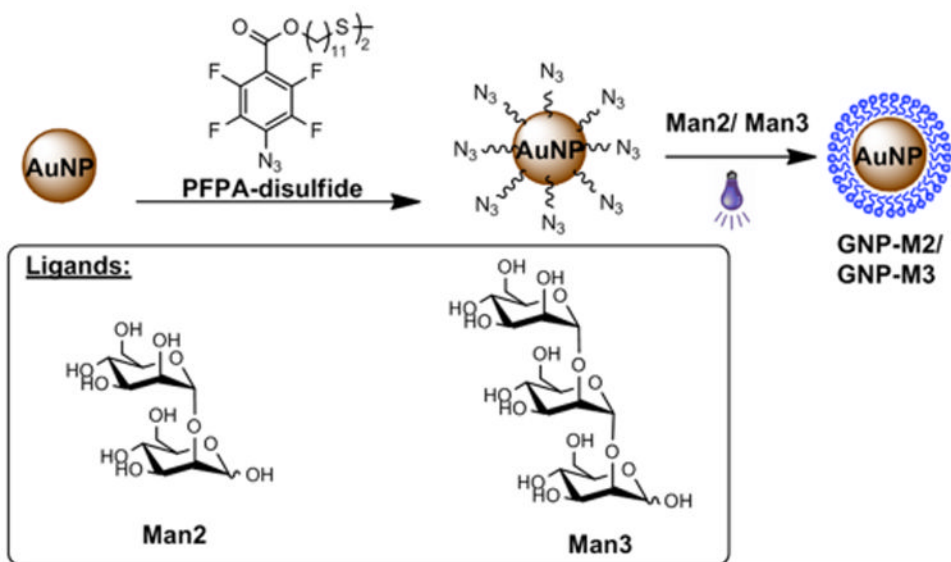


Fig. 1.
Synthesis of Man2- and Man3-conjugated AuNPs GNP-M2 and GNP-M3.

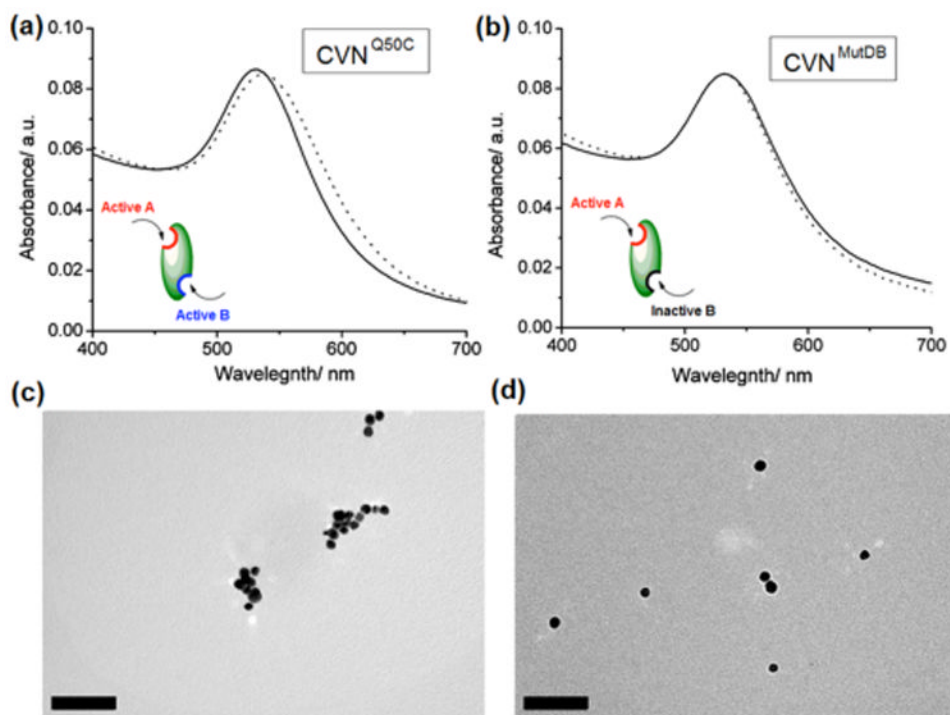


Fig. 2. UV-vis spectra of **GNP-M3** before (solid line) and after (dotted line) treatment with a) CVN^{Q50C} and b) CVN^{MutDB}. TEM micrographs of **GNP-M3** treated with c) CVN^{Q50C} and d) CVN^{MutDB}. Scale bars: 100 nm.

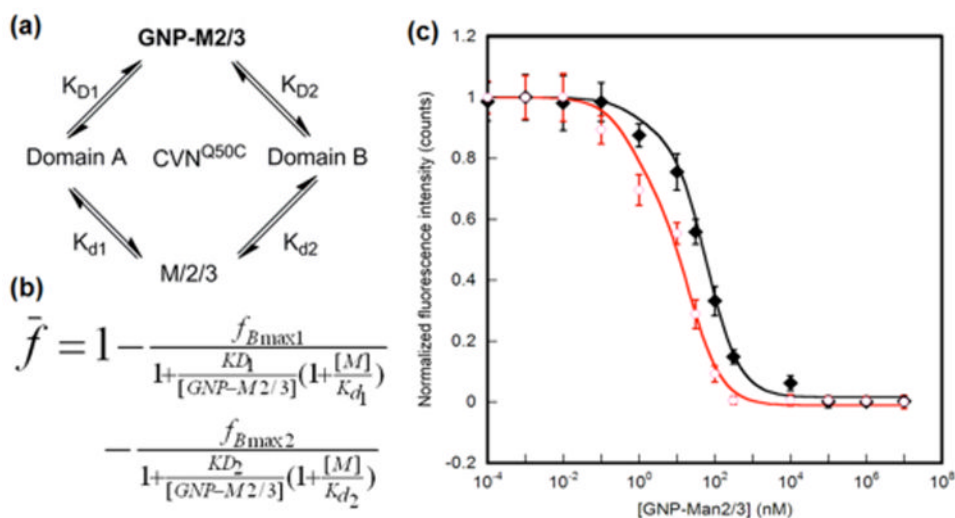


Fig. 3. Fluorescence competition assay. a) Schematic representation of binding scenario. b) Modified Cheng-Prusoff equation based on a competitive two site binding model, where $[M]$ is the concentration of the free ligand, and K_{d1} and K_{d2} are the dissociation constants of the free ligand for the glycan-binding sites on Domains A and B of CVN^{Q50C}, respectively. The data were fitted using the maximum bound fractions, f_{Bmax1} and f_{Bmax2} , corresponding to the two binding sites, and dissociation constants K_{D1} and K_{D2} as adjustable parameters. c) Concentration response curves of GNP-M2 and GNP-M3.

Table 1

Affinities for Man2/3 (K_d) and **GNP-M2/3** (K_D) binding to CVN^{Q50C}. Numbers in parentheses correspond to EF ($=K_{d1}/K_{D1}$ ·Number of ligands on GNP).

| Ligand | K_{d1} or K_{D1} (Domain A) | K_{d2} or K_{D2} (Domain B) |
|---------------|---------------------------------|---------------------------------|
| Man2 | 700 ± 50 μ M | 64 ± 4 μ M |
| GNP-M2 | 56.4 ± 7 nM (8.2) | 0.24 ± 0.1 nM (176) |
| Man3 | 3.4 ± 0.2 μ M | 43 ± 2 μ M |
| GNP-M3 | 0.011 ± 0.007 nM (309) | 11.8 ± 2.3 nM (3.6) |